

# Combining Small-Volume Metabolomic and Transcriptomic Approaches for Assessing Brain Chemistry

Ann M. Knolhoff,<sup>†</sup> Katherine M. Nautiyal,<sup>‡</sup> Peter Nemes,<sup>†</sup> Sergey Kalachikov,<sup>§</sup> Irina Morozova,<sup>§</sup> Rae Silver,<sup>‡,||,⊥</sup> and Jonathan V. Sweedler<sup>\*,†</sup>

<sup>†</sup>Department of Chemistry and the Beckman Institute, University of Illinois, Urbana, Illinois 61801, United States

<sup>‡</sup>Department of Psychology, Columbia University, New York, New York 10027, United States

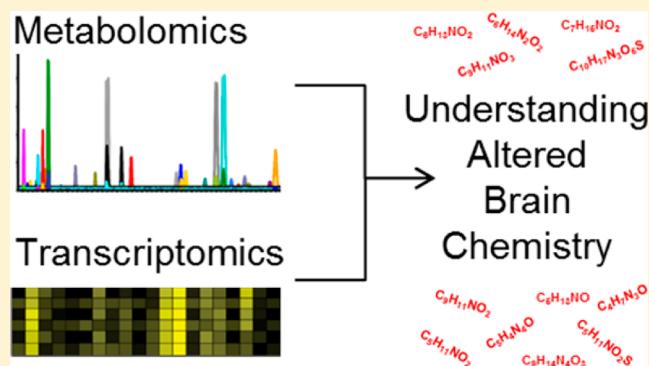
<sup>§</sup>Department of Chemical Engineering and Columbia Genome Center, Columbia University, New York, New York 10027, United States

<sup>||</sup>Department of Psychology, Barnard College, New York, New York 10027, United States

<sup>⊥</sup>Department of Pathology and Cell Biology, Columbia University, New York, New York 10032, United States

## Supporting Information

**ABSTRACT:** The integration of disparate data types provides a more complete picture of complex biological systems. Here we combine small-volume metabolomic and transcriptomic platforms to determine subtle chemical changes and to link metabolites and genes to biochemical pathways. Capillary electrophoresis–mass spectrometry (CE–MS) and whole-genome gene expression arrays, aided by integrative pathway analysis, were utilized to survey metabolomic/transcriptomic hippocampal neurochemistry. We measured changes in individual hippocampi from the mast cell mutant mouse strain, C57BL/6 *Kit*<sup>W-sh/W-sh</sup>. These mice have a naturally occurring mutation in the white spotting locus that causes reduced c-Kit receptor expression and an inability of mast cells to differentiate from their hematopoietic progenitors. Compared with their littermates, the mast cell-deficient mice have profound deficits in spatial learning, memory, and neurogenesis. A total of 18 distinct metabolites were identified in the hippocampus that discriminated between the C57BL/6 *Kit*<sup>W-sh/W-sh</sup> and control mice. The combined analysis of metabolite and gene expression changes revealed a number of altered pathways. Importantly, results from both platforms indicated that multiple pathways are impacted, including amino acid metabolism, increasing the confidence in each approach. Because the CE–MS and expression profiling are both amenable to small-volume analysis, this integrated analysis is applicable to a range of volume-limited biological systems.



With their littermates, the mast cell-deficient mice have profound deficits in spatial learning, memory, and neurogenesis. A total of 18 distinct metabolites were identified in the hippocampus that discriminated between the C57BL/6 *Kit*<sup>W-sh/W-sh</sup> and control mice. The combined analysis of metabolite and gene expression changes revealed a number of altered pathways. Importantly, results from both platforms indicated that multiple pathways are impacted, including amino acid metabolism, increasing the confidence in each approach. Because the CE–MS and expression profiling are both amenable to small-volume analysis, this integrated analysis is applicable to a range of volume-limited biological systems.

transcriptomics adaptable to small-volume samples, such as defined regions in the CNS.<sup>5,9</sup> The combination of metabolomic and transcriptomic data should yield a more complete view of the chemistry of the biological system of interest.

Here we integrate metabolomic and transcriptomic analyses to characterize the chemical heterogeneity of the brain (see experimental workflow in Figure 1). The objective of our investigation of the CNS was to examine the chemical contribution of multifunctional immune system cells to normal and abnormal function. Mast cells are resident in the brain of mammalian species and have been implicated, along with microglia, in neuroinflammation.<sup>10</sup> In the mouse brain, mast cells are located in and near the hippocampal formation, a

**Received:** November 13, 2012

**Accepted:** February 14, 2013

**Published:** February 14, 2013

Multiple analytical approaches have been combined and used to better understand chemically complex biological processes, yielding important insights on how chemistry and biology relate to function and disease state. The integration of metabolomics and transcriptomics has proven particularly useful when studying the central nervous system (CNS), which is characterized by heterogeneous cell types and complex behavioral phenotypes. Metabolomic studies delineate the small molecule content of a given sample to reveal differences between sample types or physiological states, especially with regard to disease.<sup>1–3</sup> These measurements have been helpful in a variety of applications, such as determining molecular differences in brain tumors<sup>4</sup> and characterizing the molecular composition of single neurons.<sup>5–7</sup> Transcriptomic analyses are indispensable in brain research; for example, gene expression has been characterized in different cell types in the brain, including neurons, astrocytes, and oligodendrocytes.<sup>8</sup> Continuous progress in these fields has made both metabolomics and

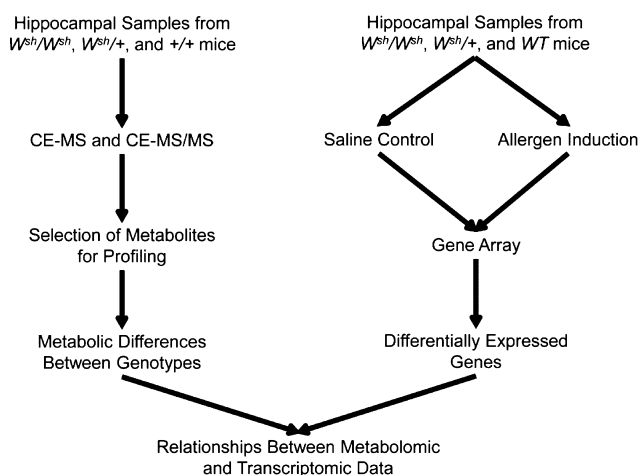


**Figure 1.** Schematic for experimental workflow: metabolomic and transcriptomic analyses were combined to enable the characterization of related chemical changes between genotypes.

structure known to modulate stress responses. Mast cells are also well-known for their role in allergic response and, more recently, have been implicated in additional innate and adaptive immune responses.<sup>11</sup> Furthermore, the population of brain mast cells fluctuates with behavioral, endocrine, and disease states.<sup>12</sup> Mast cell-deficient mice, bearing alterations in the *Kit* gene, have been used in studies of the biological functions of mast cells.<sup>13–15</sup> The c-Kit receptor (also known as the tyrosine kinase Kit receptor, stem cell growth factor receptor, or CD117) is a protein encoded by the *Kit* gene. This cytokine receptor is expressed on the surface of hematopoietic cells and binds to the stem cell factor (also known as c-Kit ligand). The reduced c-Kit receptor expression results in abnormalities in pigmentation and an inability of mast cells to differentiate from their hematopoietic progenitors.<sup>16,17</sup>

Using small-volume metabolomic and transcriptomic measurements, we examined the mast cell mutant mouse, C57BL/6 *Kit*<sup>W<sup>sh</sup>/W<sup>sh</sup></sup>. This mouse strain has an inversion upstream of the *Kit* gene that leads to mast cell deficiency due to a selective reduction of the *Kit* expression. These mice are fertile but have abnormalities in splenic myeloid and megakaryocytic hyperplasia. At the behavioral level, mast cell-deficient *Kit*<sup>W<sup>sh</sup>/W<sup>sh</sup></sup> mice have normal locomotor activity and altered anxiety-like behavior, spatial learning, and memory compared to their littermates<sup>18</sup> and have reduced neurogenesis in the hippocampal regions bearing mast cells and an altered serotonin chemistry.<sup>19</sup> Given that many other cell lineages, including hematopoietic stem and progenitor cells, red blood cells, neutrophils, intestinal pacemaker cells, melanocytes, and germ cells bear the c-Kit receptor, we sought to examine the metabolic consequences of a mutation in this receptor in the *Kit*<sup>W<sup>sh</sup>/W<sup>sh</sup></sup> mutant mouse. Because of the role of mast cells in allergy, we also examined whether allergy induction affected cells in brain regions populated by mast cells. This biological model is an ideal candidate for using a combined transcriptomics and metabolomics approach to better understand how chemistry can relate to function, especially with regard to the observed behavioral phenotypes.

In order to understand the impact of the c-Kit mutation on the overall metabolic state of the hippocampus, we studied hippocampal chemistry. Taking a systems biology approach, metabolic and cell-to-cell signaling data were combined with

transcriptomic data to focus on the chemical alterations in the hippocampus of c-Kit mutant mice. Hippocampi from mast cell-deficient mice (*W<sup>sh</sup>/W<sup>sh</sup>*) were compared to those of their heterozygous (*W<sup>sh</sup>/+*) and homozygous littermates (*+/+*) using small-volume assays. In one set of experiments, the relative abundances of more than 40 identified metabolites were determined in tissue extracts from these three genotypes using capillary electrophoresis (CE) coupled to electrospray ionization (ESI) mass spectrometry (MS). Because of its nanoliter volume sample requirements, CE–MS is well suited for the study and determination of the differences in metabolites while allowing multiple technical replicates from each sample, even from the small-volume samples that are obtained from a specific region of individual mouse brain.<sup>6,20</sup> This instrumental platform is capable of detection limits of less than 50 nM, has a large linear dynamic concentration range, is tolerant of salty samples, and has been implemented in single-cell analyses.

In a separate experiment, transcriptomic data was collected via total RNA isolation followed by hybridization to whole-genome gene expression arrays to compare gene expression differences in the hippocampus between allergen-sensitization or saline-treatment in *W<sup>sh</sup>/+* and *W<sup>sh</sup>/W<sup>sh</sup>* littermates as well as unrelated wild-type (WT) mice. Because of the integral involvement of mast cells in allergic responses, the allergy treatment provided additional insight into a potential mast cell-mediated role in the CNS. The c-Kit mutation caused statistically significant chemical changes in the mouse hippocampus in multiple metabolite pathways that were detected by both approaches. Our results demonstrate the effectiveness of combining CE–MS metabolite data and transcript data to identify a subset of metabolic pathways altered by this mutation and confirm the applicability of this approach to chemically complex small-volume measurements.

## EXPERIMENTAL SECTION

**Chemicals.** Chemicals and reagents were from Sigma-Aldrich (St. Louis, MO) unless indicated otherwise: 1 × Hank's balanced salt solution (HBSS) without phenol red (Invitrogen, Carlsbad, CA), water (LC-MS grade, Chromosolv), methanol (Optima, Fisher Scientific, Fair Lawn, NJ), formic acid (99+%, Thermo Scientific, Rockford, IL), acetic acid (99+%), 4-(2-hydroxyethyl)-1-piperazineethanesulfonic acid (HEPES) (99.5%), and RNAlater-ICE (Ambion, Austin, TX).

**Animals.** Animal care and testing protocols were approved by the Columbia University Institutional Animal Care and Use Committee. *W<sup>sh</sup>/W<sup>sh</sup>* mice (B6.Cg-*Kit*<sup>W<sup>sh</sup></sup>/HNIhrJaeBsmJ) were originally obtained from The Jackson Laboratory (Bar Harbor, ME) and bred to establish a colony at the Columbia University animal facility. The *W<sup>sh</sup>/W<sup>sh</sup>* mice were crossed with WT C57BL/6 mice (Jackson Laboratory) to generate heterozygous mice (*W<sup>sh</sup>/+*). Male littermates from *W<sup>sh</sup>/+* × *W<sup>sh</sup>/+* crosses were used in these experiments and were also used to obtain homozygous (*+/+*) mice with mast cells. Genotypes were determined based on coat color, as the *W<sup>sh</sup>* mutation causes abnormalities in pigmentation.<sup>16</sup> The mutation was confirmed by staining for mast cells in the brain with toluidine blue as previously described.<sup>19</sup> Additional WT mice were purchased (C57BL/6, Charles River, Wilmington, MA) for the gene expression analysis. Litters were weaned at 28 days, and mice were housed 2–5 per cage in transparent plastic bins (36 cm × 20 cm × 20 cm) on a 12:12 light–dark cycle. Cages had corn cob bedding (Bed-o-cobs, Maumee, OH), and food and water were provided *ad libitum*.

**Sample Preparation for CE–ESI–MS.** For the CE–ESI–MS analysis, male mice (5–6 months of age) were sacrificed by rapid decapitation and the brains removed from the crania and dissected in half midsagittally. The left hemisphere was affixed to the vibratome chuck with Crazy Glue and brain slices (300  $\mu\text{m}$  thick) were sectioned in HBSS. The left caudal hippocampus was dissected and placed in extraction solution (50% methanol containing 0.5% (v/v) acetic acid) to yield a concentration of 20  $\mu\text{L}/\text{mg}$  of tissue. This extraction solution composition has been used successfully for extracting metabolites, while also preventing degradation.<sup>6,7,20</sup> Additionally, the combination of methanol and acidic pH are sufficient for quenching enzymatic processes.<sup>21</sup> These samples were grossly homogenized and then incubated for 90 min at 4 °C. The samples were centrifuged at 15 000g for 15 min, and the supernatants were transferred to polymerase chain reaction tubes to better accommodate the sample volume; the samples were frozen at –80 °C until analysis. Finally, an internal standard, 4-(2-hydroxyethyl)-1-piperazineethanesulfonic acid (HEPES), was added to the sample extracts for a final concentration of 1  $\mu\text{M}$ . The number of biological replicates was 10 for  $W^{sh}/W^{sh}$ , 9 for  $W^{sh}/+$ , and 5 for  $+/+$ .

**CE–ESI–MS.** The metabolomics measurements were performed with a custom-designed CE–ESI–MS instrument platform, similar to the one previously used<sup>6</sup> and described in detail elsewhere.<sup>7,22</sup> Briefly, a sample volume of 6 nL was hydrodynamically injected into a separation capillary having the following dimensions: 40  $\mu\text{m}$  inner diameter, 105  $\mu\text{m}$  outer diameter, and 90 cm in length (Polymicro Technologies, Phoenix, AZ). The CE conditions used were 20 kV for the separation voltage and 1% formic acid for the background electrolyte. A coaxial sheath flow interface was used to hyphenate the CE system to the mass spectrometer. A sheath flow consisting of 50% methanol with 0.1% (v/v) formic acid was introduced at a rate of 750 nL/min. Generated ions were measured by an orthogonal time-of-flight mass spectrometer (micrOTOF ESI-TOF, Bruker Daltonics, Billerica, MA), and tandem MS (MS/MS) experiments were performed with a high-resolution mass spectrometer (maXis ESI-Qq-TOF, Bruker Daltonics). Three technical replicates were analyzed for each sample.

**CE–ESI–MS Data Analysis.** The molecular content of the mouse hippocampus extracts was determined via manual data analysis using the mass spectrometer software, DataAnalysis (Bruker Daltonics). Extracted ion chromatograms were plotted from  $m/z$  50 to 500 with a 500 mDa window. When an eluting peak was observed, the accurate mass of the ion was registered and searched against the Scripps metabolite database, METLIN.<sup>23</sup> Accurate mass calculations were performed using a molecular weight calculator, which is free, downloadable software from the Pacific Northwest National Laboratory [<http://omics.pnl.gov/software/MWCalculator.php>]. The MS/MS data obtained from the sample was compared against fragmentation data listed in METLIN when available. Chemical standards were also analyzed to improve the confidence of analyte identification by evaluating the MS/MS data and migration time of these compounds.

Relative metabolite levels were assessed and compared among hippocampus extracts. Selected ion electropherograms were generated with a 10 mDa window for a selected array of metabolites, and the intensities of the detected peaks were noted. For some high intensity signals, the intensity of the A + 1 peak was evaluated in addition to the monoisotopic ion to

avoid detection biases due to potential saturation of the detector in the mass spectrometer. Measured intensities were normalized with respect to the peak intensity of the internal standard, HEPES. The normalized peak intensity of each identified analyte was averaged among the technical replicates, and the obtained values were statistically evaluated with the Student's t-test using a two-tailed distribution with two-sample equal variance (homoscedastic) in Excel (Microsoft, Redmond, WA). In this work, a calculated  $p$ -value of  $\leq 0.05$  was considered to indicate statistically significant differences between data groups.

**Gene Array.** For the gene array studies, mice were sacrificed by decapitation and brains were rapidly removed from the crania, flash frozen in liquid nitrogen, and then transferred to a cryostat kept at –20 °C. Brains were sectioned in the coronal plane at a thickness of 100  $\mu\text{m}$ . Four hippocampi were dissected out of two adjacent sections, and tissue was pooled in 0.5 mL of RNAlater-ICE, precooled to –20 °C. Following storage for 24 h at –20 °C, the RNAlater-ICE was removed and the tissue sample frozen at –80 °C until further processing. Total RNA was isolated using RNAqueous Micro RNA (Life Technologies, Grand Island, NY) isolation kits. RNA was quantified with a Quant-IT RNA fluorometric assay (Life Technologies) and checked for integrity using the Bioanalyzer (Agilent, Palo Alto, CA). The resulting RNA samples were amplified using a conventional *in vitro* transcription-mediated linear amplification procedure (MessageAmp II, Life Technologies), reciprocally labeled with AlexaFluor 546 or AlexaFluor 647 (Life Technologies) for induced allergy and control samples and hybridized to mouse whole-genome gene expression arrays (SurePrint G3Mouse GE 8x60K Kit, Agilent).

The raw signal intensity data was filtered for background and technical outliers, normalized for dye and array effects using the *loess* normalization procedure implemented by the Bioconductor package *affy*,<sup>24</sup> and compared for differential gene expression using hypothesis testing statistics similar to those previously described.<sup>25,26</sup> The data were further corrected for type 2 error using Storey's false discovery rates (FDR)<sup>27</sup> and appropriate statistical packages and subroutines implemented in R<sup>28</sup> and Bioconductor.<sup>29</sup> Genes differentially expressed between the groups were selected at  $<0.5\%$  FDR (typically one to three expected false-positives per set) and a more than 2-fold change in expression. Differences in the genes of interest related to the CE–ESI–MS data were isolated from the data set, with a specific focus on genes in the choline and autophagy pathways. The hierarchical clustering was performed in Spotfire Suite for Functional Genomics (TIBCO Spotfire, Inc., Somerville, MA) using the unweighted pair group method with arithmetic mean (UPGMA) as a clustering method with Euclidean distance as the similarity measure.<sup>30</sup>

**Allergy Induction.** For the gene microarray study, WT mice and  $W^{sh}/+$  and  $W^{sh}/W^{sh}$  littermates were exposed to allergen or saline treatment. Induction of allergy was performed as previously described.<sup>31</sup> Briefly, mice were injected with ovalbumin (10  $\mu\text{g}$ ; Sigma Aldrich) in Imject Alum (2 mg/mL; Pierce, Rockford, IL) or with the equivalent volume of saline (0.5 mL) via intraperitoneal injection. After 14 days, mice were challenged four times every 48 h with an intranasal injection of ovalbumin (10  $\mu\text{g}$  in 8  $\mu\text{L}$  of saline) or saline (8  $\mu\text{L}$ ). At a time of 24 h following the last intranasal injection, the mice were sacrificed. Trunk blood collected at this time confirmed an increase in Immunoglobulin E in allergy-treated animals (data not shown).

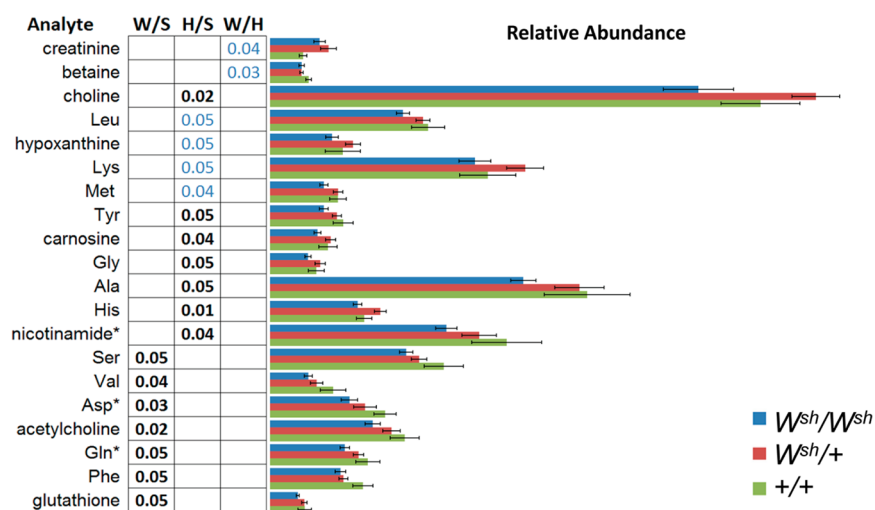


**Figure 2.** Metabolites with significant differences in relative abundance in pairwise comparisons of  $W^{sh}/W^{sh}$ ,  $W^{sh}/+$ , and  $+/+$  mice. Bars show the mean of normalized abundances measured in the biological replicates for each genotype; error bars represent standard error;  $p$ -values from the corresponding Student's  $t$ -tests are tabulated to the left. Statistically significant differences in the levels of these analytes ( $p \leq 0.05$ ) are also supported by gene expression data. Metabolites associated with differentially expressed metabolic pathways identified by gene expression analysis are marked with black bold in the table. An asterisk indicates that the intensity is reflective of the second peak in the isotopic series due to its high concentration. Key: WT (W),  $W^{sh}/+$  (H),  $W^{sh}/W^{sh}$  (S).

**Safety Considerations.** Standard safety protocols were implemented when handling animals, samples, and solvents. The high voltage and electrically conductive connections of the CE–ESI-MS platform were grounded or shielded.

## RESULTS AND DISCUSSION

The combination of approaches used in this study permits two parallel analyses of the neurochemical pathways associated with genetic and metabolic changes that arise in several brain regions of the c-Kit mutant mouse (Figure 1). These changes were appreciable in spite of substantial interindividual variation, variation within individuals over time, and variations in the numbers of mast cells present. The analytes measured via CE–MS are listed in Table S1 in the Supporting Information). A number of global chemical differences were observed between  $W^{sh}/W^{sh}$  and  $W^{sh}/+$  and  $+/+$  mice, and additionally between  $W^{sh}/W^{sh}$  and  $W^{sh}/+$  and WT mice (Table S2 in the Supporting Information). It is noteworthy that at the gross anatomical level, the brains of these mice appear normal, even though the metabolic evidence from our investigations points to extensive chemical changes accompanying the mutation. There are minor differences in volume in the dentate gyrus region of the hippocampus, but overall there are no large morphological differences in the hippocampus of  $W^{sh}/W^{sh}$  mice as previously reported.<sup>19</sup>

**Metabolomic and Transcriptomic Analyses.** Several hundred distinct ions were detected for each hippocampal sample, but only those signals that were assigned to specific metabolites with high confidence using a combination of accurate mass, retention time, and fragmentation data, and that were detected in most samples were used in subsequent analyses. Thus, the relative abundances of 42 measured analytes were determined and statistically evaluated in a pairwise comparison for the hippocampus extracts from  $W^{sh}/W^{sh}$ ,  $W^{sh}/+$ , and  $+/+$  mice. A total of 20 distinct analytes exhibited statistically significant differences in relative abundance (Figure 2), with these molecules consisting of amino acids, classical neurotransmitters, and nucleosides. In particular, 11 different

analytes were present in significantly different amounts between the  $W^{sh}/W^{sh}$  and  $W^{sh}/+$  mice ( $p$ -value  $\leq 0.05$ ), including multiple amino acids, choline, nicotinamide, hypoxanthine, and carnosine. In general, the  $W^{sh}/W^{sh}$  mice had lower relative analyte concentrations when compared to their heterozygous littermates (e.g., histidine, choline, and various amino acids). The  $+/+$  mice were also analyzed; some metabolites exhibited the same trends observed in the  $W^{sh}/W^{sh}$  and  $W^{sh}/+$  comparison, while others did not. For example, the  $+/+$  mice had lower levels of creatinine in comparison with the other two genotypes, and the  $W^{sh}/W^{sh}$  and  $W^{sh}/+$  mice had comparable levels of betaine, but higher concentrations were observed in the  $+/+$  counterparts. Furthermore, seven analyte levels were statistically lower in the  $W^{sh}/W^{sh}$  when compared to the  $+/+$  mice, including acetylcholine, glutathione, and a few additional amino acids (Figure 2). While graded concentration levels for a number of analytes were observed ( $W^{sh}/W^{sh} < W^{sh}/+ < +/+$ ), these often did not rise to the point of statistical significance for all genotypes studied (Figure 2; e.g., serine and valine were statistically different in the  $W^{sh}/W^{sh}$  and  $W^{sh}/+$  comparison but not for the  $W^{sh}/+$  and  $+/+$  comparison).

The observed metabolite changes were supplemented with transcriptomic measurements to further characterize the chemistry of the sample; specifically, differences in gene expression were determined in the hippocampal samples from  $W^{sh}/W^{sh}$  and  $W^{sh}/+$  mice. Furthermore, because mast cells are known to be intimately involved in allergic responses, gene expression data was also collected and analyzed for mice exposed to either an allergen or a saline control. The accumulated data revealed that differentially expressed genes appeared to be related to the observed changes in metabolites; therefore, the corresponding expression and metabolite data were further examined to assess the relationships between the metabolic pathways that included the differentially expressed genes and those associated with altered mast cell composition. The gene expression data was analyzed for various pairwise combinations in a  $2 \times 2$  experimental design ( $W^{sh}/W^{sh}$  versus  $W^{sh}/+$  animals, treated with either saline or allergen). These

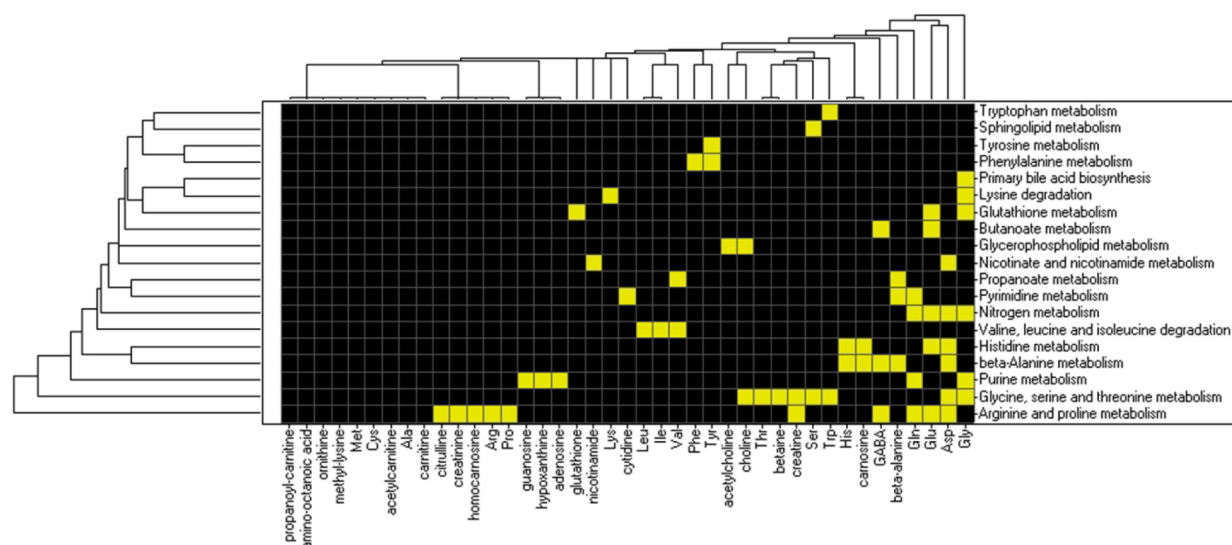


**Figure 3.** Hierarchical clustering of affected metabolites based on their participation in pathways containing differentially expressed genes. Pathways (rows) were clustered against metabolites (columns) monitored by CE-ESI-MS using the UPGMA clustering algorithm with the Euclidean distance as a similarity measure. A yellow block in the diagram indicates that a given metabolite is involved in the corresponding pathway containing mast cell-associated genes found through the expression analysis.

comparisons were indicative of changes in gene expression as a consequence of the c-Kit mutation. In the pairwise comparison, 21 differentially expressed genes were found to be associated with pathways that are involved with changing metabolites.

Among the c-Kit associated-metabolite pathway-related (CA-MPR) genes were those coding for acetylcholinesterase, pyruvate dehydrogenase (lipoamide) beta, and genes involved in autophagy (Table S3 in the Supporting Information). In particular, 19 CA-MPR genes had significantly different expression levels between the  $W^{sh}/W^{sh}$  and  $W^{sh}/+$  mice, both treated with an allergen. When extending this analysis to also include the WT mice (Table S3 in the Supporting Information), 50 differentially expressed genes were associated with pathways involved with changing metabolites in the  $W^{sh}/W^{sh}$ ,  $W^{sh}/+$ , and  $+/+$  genotype comparison (Figure 2).

Hierarchical cluster analysis was implemented on the data to help further evaluate connections between gene expression and metabolite composition of the hippocampi. As shown in Figure 3, when comparing WT and  $W^{sh}/W^{sh}$  mice, the majority of the metabolites that varied by genotype had a matching pathway identified based solely on differential gene expression. As can also be seen from the figure, different pathways can implicate multiple metabolites; furthermore, each metabolite can participate in several pathways. Thus, with the exception of the phenylalanine/tyrosine metabolism pathways, Figure 3 may be better viewed as an interconnected metabolic super network. The clustering pattern (bottom right corner of the diagram) indicates that the network is mostly governed by changes in the arginine/proline and glycine, serine and threonine, and purine metabolism pathways. (See Table S2 in the Supporting Information for the complete listing of metabolites and affected pathways for the three genotypes.) It is remarkable that many canonical KEGG metabolic pathways associated with the metabolites noted to change in abundance were also detected by the analysis of differential gene expression in hippocampi from the same animal groups, providing a mechanistic link between the differences in animal genotypes and variations in the metabolite abundance (Figures 2 and 3). Thus, the two analytically orthogonal techniques used in combination here are

able to describe the same events at different levels of phenotypic expression, thereby independently supporting and ameliorating each other.

**Choline, Acetylcholine, and Histidine Changes.** Several metabolic pathways are consistent with the observed differences in metabolite levels and gene expression, such as choline and acetylcholine. Acetylcholinesterase gene expression was statistically different between saline-treated  $W^{sh}/W^{sh}$  and  $W^{sh}/+$  mice as well as between allergen-treated  $W^{sh}/W^{sh}$  and  $W^{sh}/+$  mice. This finding was consistent with the observed choline deficit in  $W^{sh}/W^{sh}$  mice. While there was no statistical difference for acetylcholine between  $W^{sh}/W^{sh}$  and  $W^{sh}/+$  mice, there was a statistical difference between  $W^{sh}/W^{sh}$  and  $+/+$  mice as well as a relative decrease in acetylcholine concentrations ( $W^{sh}/W^{sh} < W^{sh}/+ < +/+$ ) (see Table S4 in the Supporting Information). Differential expression of the gene for choline dehydrogenase was also observed, which could be a result of the observed lower levels of choline. Furthermore, downstream metabolite levels in this pathway were also statistically different between the genotypes (e.g., betaine and methionine). Moreover, this pathway provides a connection to the synthesis of multiple amino acids; our observed differences in amino acid levels are in agreement with this notion.

Altered choline and acetylcholine levels have been linked to several behaviors or disorders that were also observed in the mast cell-deficient mice. For example, hippocampal neurogenesis is modulated by prenatal choline availability,<sup>32</sup> which could be participating in the observed neurogenesis of the  $W^{sh}/W^{sh}$  genotype. Likewise, choline can also affect visuospatial memory as a function of choline administration<sup>33–35</sup> and affect hippocampal plasticity.<sup>36</sup> Acetylcholine is involved in a variety of functions, including learning and memory in the hippocampus.<sup>37</sup> The acetylcholine deficit can contribute to the observed defects in spatial memory and learning. Furthermore, acetylcholine release in the hippocampus in response to anxiety and stress has been documented and results in an anxiolytic effect.<sup>38–42</sup> If acetylcholine levels are impaired, this may contribute to the observed anxiety-like behavior in these mice.

Mast cells release histamine in response to acetylcholine.<sup>43,44</sup> Histamine levels were lower in the  $W^{sh}/W^{sh}$  mice compared to the  $W^{sh}/+$  littermates, confirming that mast cells contribute to brain histamine levels.<sup>18</sup> While the levels of histamine were below the limits of detection for the current instrument platform, its precursor, histidine, was measured at lower levels in  $W^{sh}/W^{sh}$  mice compared to the  $W^{sh}/+$  mice. The lack of mast cells may result in lower expression levels of these analytes in other cell types in the hippocampus because they are no longer needed to regulate mast cell release.

**Amino Acid Metabolism.** While the changes in molecules related to cell–cell signaling discussed in the previous section were expected based on the mediators released by mast cells, the decrease in many monitored amino acids in the c-Kit mice is surprising, as most pathways do not affect amino acids so indiscriminately. Depletion of amino acids can induce autophagy, a catabolic process in which cells are degraded for energy production.<sup>45</sup> In the brain, increased autophagy is observed after injury<sup>46</sup> and complete impairment of autophagy results in neurodegeneration.<sup>47,48</sup> While this scenario was not directly tested in the current work, it is possible that autophagy had been induced, which would result in a modified cellular environment. In agreement, several genes for proteins involved in autophagy were differentially expressed between the  $W^{sh}/W^{sh}$  and  $W^{sh}/+$  littermates (Table S3 in the Supporting Information; Ras proteins).

Another possible reason for the amino acid-level changes may be related to the pyruvate dehydrogenase beta (*Pdhb*) gene; this gene is differentially expressed in  $W^{sh}/W^{sh}$  versus  $W^{sh}/+$  mice after allergen treatment. *Pdhb* participates in the citrate, or Krebs, cycle and so is involved in multiple amino acid pathways. *Pdhb* is also involved in pyruvate metabolism, which is connected to nicotinamide metabolism, the biosynthesis of several amino acids including lysine, and is directly involved in leucine biosynthesis. Additionally, the nicotinamide pathway is included under the affected pathway list determined by the gene expression analysis (Figure 3). Such dysregulation of *Pdhb* expression could be responsible for the decrease in multiple amino acids and nicotinamide observed in the  $W^{sh}/W^{sh}$  mice as compared to the  $W^{sh}/+$  littermates.

**Additional Altered Pathways.** Some of the differences between *Kit* mutant and WT animals are not directly involved with the repertoire of chemical mediators that are localized within mast cell granules. Instead they implicate targets of mast cell mediators (i.e., chemicals released by mast cells that act on other parenchymal elements). For the gene expression analysis, particular attention was focused on mining the data for differences in expression related to the metabolite changes described in the CE–ESI–MS analyses.

Pathway analysis revealed that the mast cell-dependent metabolites and mast cell-associated differentially expressed genes share many of the same pathways. Using hierarchical clustering analysis, metabolites were grouped based on their participation in metabolic pathways that included differentially expressed genes (Figure 3). It was observed that the majority of affected pathways and metabolites were connected either by shared pathways or by their products, forming a single network. This was true despite the use of unrelated control mice (WT and  $+/+$ ). It may be inferred from the data that the majority of the metabolite changes may be regulated by changes in gene expression of a handful of pathways, seen at the bottom of the diagram. The exact details of such regulation may be a tempting subject for a follow-up study.

Several pathway/metabolite combinations are intriguing, given what is known about mast cell function within the brain. For example, the *Pdhb* gene is differentially expressed in a mast cell-dependent manner and has been shown to increase in the rat hippocampus after chronic antidepressant treatments (like serotonin), in addition to other proteins that are associated with neurogenesis.<sup>49</sup> Stress has also been shown to suppress hippocampal neurogenesis, which is mediated by interleukin-1,<sup>50,51</sup> a cytokine that mast cells synthesize.<sup>52</sup> As noted in an independent study,  $W^{sh}/W^{sh}$  mice exhibit heightened anxiety-like behavior.<sup>18</sup>

Similarly, stress has resulted in amino acid level changes in various biological sample matrixes. For example, amino acids have been found to change in blood plasma, urine, and regions of the brain as a result of stress;<sup>53–58</sup> furthermore, some murine models of chronic stress also demonstrate severe immunosuppression,<sup>59,60</sup> which could be mediated by mast cells. Additional support for a link between mast cells and stress is that chronic stress results in increased numbers of mast cells in the CNS.<sup>61</sup> Stress can also induce increased permeability of the blood–brain–barrier through mast cell activation,<sup>62,63</sup> which could be responsible for molecular differences.

*Kit* mutant animals are well-known for their augmented response to allergens. Thus, it was interesting to see whether genes associated with the metabolic differences found between  $W^{sh}$  and  $+/+$  animals are differentially expressed during the allergic reaction in a *Kit*-dependent manner. These genes and their association with a particular metabolite and its expression are shown in Table S3 in the Supporting Information. It is remarkable that in addition to the genes apparently associated with metabolic pathways and specific metabolites, many of the metabolites in turn are associated with neuroligand receptor interaction pathways. These include *Crhr1*, *Aplnr*, *Gabra2*, *Scrr1*, *Drd2*, and signal transduction pathways and global transcription regulators such as *Nkiras2*, *Ras110a*, *Mapk1*, and *Dvl2*.

### Mast Cells in Behavioral and Physiological Systems.

The combined cell count of neurons, glia, and microglia in the mouse hippocampus is greater than one million,<sup>64–68</sup> while mast cells are far fewer in number. The entire mouse brain is estimated to contain an average of 500 mast cells, with a range of 180–709 mast cells per individual in the mouse strain studied in our work.<sup>69</sup> In contrast to resting microglia however, mast cells constantly release their granular material, even at rest. Their population is mobile, and they can be rapidly recruited in response to normal physiological signals and following immune system activation.<sup>12,70–72</sup> Furthermore, mast cells are present and actively release their granular material throughout development. In this context, it may not be surprising that large-scale metabolite differences are observed between  $W^{sh}/W^{sh}$  and  $W^{sh}/+$  mice. While some of the metabolites present in mast cells may be distinct from those in other brain cells (e.g., neurons, glia, and endothelial cells), the greater than 3 orders of magnitude difference in cell-type abundance and the ubiquitous nature of the metabolites with affected levels (e.g., the amino acids) indicates that the majority of changes are in metabolites external to mast cells. Thus, this mutation, and likely the lack of mast cells, appears to affect large numbers of hippocampal cells. Mast cell granules have many potent mediators, and these released mediators can migrate over great distances.<sup>18,73,74</sup> Perhaps the observed chemical changes are a result of volume transmission, an intracellular mode of communication that potentially affects and modulates the activity of entire brain

regions.<sup>75</sup> Another possibility is that the deficits are attributable to the cumulative effect throughout development of the *Kit* mutation or the mast cell deficit. Some aspects previously attributed to the mast cell deficit may turn out to be due to the disrupted *Kit* receptor. The development of mice deficient in mast cells independent of alterations in the *Kit* receptor<sup>76</sup> will enable the examination of whether this receptor might contribute to the losses described herein.

## CONCLUSIONS

The combination of CE–MS-based metabolomics and whole genome transcriptomics approaches enabled us to determine chemical changes and understand how they relate to an observed phenotype. In *c-Kit* mutant mice, there is a striking global chemical difference in the hippocampus metabolite content, which may be caused by changes in the hippocampal cell chemical content consequent to loss of mast cells or of the *Kit* receptor. A drastic chemical effect is observed in both the brain metabolic profile and in a remarkable range of pathways. The magnitude of these molecular changes is surprising given the relatively small number (and fraction) of mast cells in the brain. It is intriguing to speculate how these changes correlate to the observed behavioral and developmental differences observed in *Kit* mutant mice.<sup>19</sup> Compounds of particular interest include choline, with its link to memory and neurogenesis, as well as acetylcholine and its relationship to stress, learning, and memory. Less straightforward to interpret is the decrease in abundance of multiple amino acids. There may be a cumulative developmental link, which is suggested by prior studies highlighting a significant decrease in neurogenesis observed in mast cell-deficient mice.<sup>19</sup> Furthermore, the possibility of aggregating the pathways and metabolites via hierarchical clustering suggests that the majority of the pathways form a single interconnected network based on the metabolites common to both. Regardless, these global chemical differences provide a framework for follow-up experiments to obtain specific mechanistic information, as well as to understand how specific cell types such as neurons and glia are affected. The combination of metabolomic and transcriptomic measurements allows us to highlight pathways common to both platforms, thus producing a small but validated list of metabolic pathways on which to focus future studies; as both approaches are information rich and compatible with a range of sample sizes down to individual brain nuclei, this approach offers potential for a number of brain studies.

## ASSOCIATED CONTENT

### Supporting Information

Supporting tables (Tables S1–S4) as noted in the text. This material is available free of charge via the Internet at <http://pubs.acs.org>.

## AUTHOR INFORMATION

### Corresponding Author

\*Phone: +1 217-244-7359. Fax: +1 217-244-8068. E-mail: [jsweedle@illinois.edu](mailto:jsweedle@illinois.edu).

### Notes

The authors declare no competing financial interest.

## ACKNOWLEDGMENTS

This work was supported by Award No. P30 DA081310 from the National Institute on Drug Abuse and Award No. SR01

DE018866 from the National Institute of Dental and Craniofacial Research and the Office of Director, National Institutes of Health (J.V.S.); NIH training Grant F31 MH084384 (K.M.N.); Award No. IOS 05-54514 from the National Science Foundation; and Award No. R21 MH 067782 from the National Institute of Mental Health (R.S.). The content is solely the responsibility of the authors and does not necessarily represent the official views of the awarding agencies. The molecular weight calculator was supported by the NIH National Center for Research Resources (Grant RR018522) and the W.R. Wiley Environmental Molecular Science Laboratory, a national scientific user facility sponsored by the U.S. Department of Energy's Office of Biological and Environmental Research and located at Pacific Northwest National Laboratory, which is operated by the Battelle Memorial Institute for the U.S. Department of Energy under Contract DE-AC05-76RL0 1830. The authors thank Christine Cecala for helpful discussions regarding data analysis, Jaquelyn Jahn for her technical assistance, and Stephanie Baker for assistance in the preparation of this manuscript.

## REFERENCES

- (1) Suhre, K.; Meisinger, C.; Doring, A.; Altmaier, E.; Belcredi, P.; Gieger, C.; Chang, D.; Milburn, M. V.; Gall, W. E.; Weinberger, K. M.; Mewes, H. W.; Hrabe de Angelis, M.; Wichmann, H. E.; Kronenberg, F.; Adamski, J.; Illig, T. *PLoS One* **2010**, *5*, e13953.
- (2) Wang, Z.; Klipfell, E.; Bennett, B. J.; Koeth, R.; Levison, B. S.; Dugar, B.; Feldstein, A. E.; Britt, E. B.; Fu, X.; Chung, Y. M.; Wu, Y.; Schauer, P.; Smith, J. D.; Allayee, H.; Tang, W. H.; DiDonato, J. A.; Lusis, A. J.; Hazen, S. L. *Nature* **2011**, *472*, 57–63.
- (3) Wuolikainen, A.; Moritz, T.; Marklund, S. L.; Antti, H.; Andersen, P. M. *PLoS One* **2011**, *6*, e17947.
- (4) Griffin, J. L.; Kauppinen, R. A. *FEBS J.* **2007**, *274*, 1132–1139.
- (5) Rubakhin, S. S.; Romanova, E. V.; Nemes, P.; Sweedler, J. V. *Nat. Methods* **2011**, *8*, S20–S29.
- (6) Lapainis, T.; Rubakhin, S. S.; Sweedler, J. V. *Anal. Chem.* **2009**, *81*, 5858–5864.
- (7) Nemes, P.; Knolhoff, A. M.; Rubakhin, S. S.; Sweedler, J. V. *Anal. Chem.* **2011**, *83*, 6810–6817.
- (8) Cahoy, J. D.; Emery, B.; Kaushal, A.; Foo, L. C.; Zamanian, J. L.; Christopherson, K. S.; Xing, Y.; Lubischer, J. L.; Krieg, P. A.; Krupenko, S. A.; Thompson, W. J.; Barres, B. A. *J. Neurosci.* **2008**, *28*, 264–278.
- (9) Heinemann, M.; Zenobi, R. *Curr. Opin. Biotechnol.* **2011**, *22*, 26–31.
- (10) Skaper, S. D.; Giusti, P.; Facci, L. *FASEB J.* **2012**, *26*, 3103–3117.
- (11) Shelburne, C. P.; Abraham, S. N. *Adv. Exp. Med. Biol.* **2011**, *716*, 162–185.
- (12) Silver, R.; Silverman, A.-J.; Vitkovic, L.; Lederhendler, I. I. *Trends Neurosci.* **1996**, *19*, 25–31.
- (13) Maurer, M.; Wedemeyer, J.; Metz, M.; Piliponsky, A. M.; Weller, K.; Chatterjea, D.; Clouthier, D. E.; Yanagisawa, M. M.; Tsai, M.; Galli, S. J. *Nature* **2004**, *432*, 512–516.
- (14) Soucek, L.; Lawlor, E. R.; Soto, D.; Shchors, K.; Swigart, L. B.; Evan, G. I. *Nat. Med.* **2007**, *13*, 1211–1218.
- (15) Tsai, M.; Grimbaldston, M. A.; Yu, M.; Tam, S. Y.; Galli, S. J. *Chem. Immunol. Allergy* **2005**, *87*, 179–197.
- (16) Chen, C.-C.; Grimbaldston, M. A.; Tsai, M.; Weissman, I. L.; Galli, S. J. *Proc. Natl. Acad. Sci. U.S.A.* **2005**, *102*, 11408–11413.
- (17) Kitamura, Y.; Fujita, J. *BioEssays* **1989**, *10*, 193–196.
- (18) Nautiyal, K. M.; Ribeiro, A. C.; Pfaff, D. W.; Silver, R. *Proc. Natl. Acad. Sci. U.S.A.* **2008**, *105*, 18053–18057.
- (19) Nautiyal, K. M.; Dailey, C. A.; Jahn, J. L.; Rodriguez, E.; Son, N. H.; Sweedler, J. V.; Silver, R. *Eur. J. Neurosci.* **2012**, *36*, 2347–2359.
- (20) Nemes, P.; Knolhoff, A. M.; Rubakhin, S. S.; Sweedler, J. V. *ACS Chem. Neurosci.* **2012**, *3*, 782–792.

- (21) Álvarez-Sánchez, B.; Priego-Capote, F.; Luque de Castro, M. D. *TrAC, Trends Anal. Chem.* **2010**, *29*, 120–127.
- (22) Knollhoff, A. M.; Nemes, P.; Rubakhin, S. S.; Sweedler, J. V. In *Methodologies for Metabolomics: Experimental Strategies and Techniques*; Lutz, N., Wevers, R., Sweedler, J. V., Eds.; Cambridge University Press: New York, 2013; pp 119–139.
- (23) Smith, C. A.; O'Maille, G.; Want, E. J.; Qin, C.; Trauger, S. A.; Brandon, T. R.; Custodio, D. E.; Abagyan, R.; Siuzdak, G. *Ther. Drug Monit.* **2005**, *27*, 747–751.
- (24) Gautier, L.; Cope, L.; Bolstad, B. M.; Irizarry, R. A. *Bioinformatics* **2004**, *20*, 307–315.
- (25) Sharma, A.; Zhao, J.; Podolsky, R.; McIndoe, R. A. *Bioinformatics* **2010**, *26*, 1465–1467.
- (26) Tusher, V. G.; Tibshirani, R.; Chu, G. *Proc. Natl. Acad. Sci. U.S.A.* **2001**, *98*, 5116–5121.
- (27) Storey, J. D.; Tibshirani, R. *Proc. Natl. Acad. Sci. U.S.A.* **2003**, *100*, 9440–9445.
- (28) R Core Development Team. In *R: A Language and Environment for Statistical Computing*; R Foundation for Statistical Computing: Vienna, Austria, 2011.
- (29) Reimers, M.; Carey, V. J. In *Methods in Enzymology*; Kimmel, A., Oliver, B., Academic Press: Amsterdam, The Netherlands, 2006; Vol. 411, pp 119–134.
- (30) Murtagh, F. *Comput. Stat. Q.* **1984**, *1*, 101–113.
- (31) Mayr, S. I.; Zuberi, R. I.; Zhang, M.; de Sousa-Hitzler, J.; Ngo, K.; Kuwabara, Y.; Yu, L.; Fung-Leung, W.-P.; Liu, F.-T. *J. Immunol.* **2002**, *169*, 2061–2068.
- (32) Glenn, M. J.; Gibson, E. M.; Kirby, E. D.; Mellott, T. J.; Blusztajn, J. K.; Williams, C. L. *Eur. J. Neurosci.* **2007**, *25*, 2473–2482.
- (33) Meck, W.; Smith, R.; Williams, C. *Behav. Neurosci.* **1989**, *103*, 1234–1241.
- (34) Meck, W. H.; Smith, R. A.; Williams, C. L. *Dev. Psychobiol.* **1988**, *21*, 339–353.
- (35) Meck, W. H.; Williams, C. L. *Neurosci. Biobehav. Rev.* **2003**, *27*, 385–399.
- (36) Wong-Goodrich, S. J. E.; Glenn, M. J.; Mellott, T. J.; Blusztajn, J. K.; Meck, W. H.; Williams, C. L. *Brain Res.* **2008**, *1237*, 153–166.
- (37) Hasselmo, M. E. *Curr. Opin. Neurobiol.* **2006**, *16*, 710–715.
- (38) File, S. E.; Gonzalez, L. E.; Andrews, N. *Behav. Neurosci.* **1998**, *112*, 352–359.
- (39) File, S. E.; Kenny, P. J.; Cheeta, S. *Pharmacol., Biochem. Behav.* **2000**, *66*, 65–72.
- (40) Gilad, G. M. *Psychoneuroendocrinology* **1987**, *12*, 167–184.
- (41) Imperato, A.; Puglisi-Allegra, S.; Casolini, P.; Angelucci, L. *Brain Res.* **1991**, *538*, 111–117.
- (42) Mark, G. P.; Rada, P. V.; Shors, T. J. *Neuroscience* **1996**, *74*, 767–774.
- (43) Blandina, P.; Fantozzi, R.; Mannaioni, P. F.; Masini, E. *J. Physiol.* **1980**, *301*, 281–293.
- (44) Fantozzi, R.; Masini, E.; Blandina, P.; Mannaioni, P. F.; Bani-Sacchi, T. *Nature* **1978**, *273*, 473–474.
- (45) Rabinowitz, J. D.; White, E. *Science* **2010**, *330*, 1344–1348.
- (46) Smith, C. M.; Chen, Y.; Sullivan, M. L.; Kochanek, P. M.; Clark, R. S. *Neurobiol. Dis.* **2010**, *43*, 52–59.
- (47) Hara, T.; Nakamura, K.; Matsui, M.; Yamamoto, A.; Nakahara, Y.; Suzuki-Migishima, R.; Yokoyama, M.; Mishima, K.; Saito, I.; Okano, H.; Mizushima, N. *Nature* **2006**, *441*, 885–889.
- (48) Komatsu, M.; Waguri, S.; Chiba, T.; Murata, S.; Iwata, J.; Tanida, I.; Ueno, T.; Koike, M.; Uchiyama, Y.; Kominami, E.; Tanaka, K. *Nature* **2006**, *441*, 880–884.
- (49) Khawaja, X.; Xu, J.; Liang, J.-J.; Barrett, J. E. *J. Neurosci. Res.* **2004**, *75*, 451–460.
- (50) Goshen, I.; Kreisel, T.; Ben-Menachem-Zidon, O.; Licht, T.; Weidenfeld, J.; Ben-Hur, T.; Yirmiya, R. *Mol. Psychiatry* **2008**, *13*, 717–728.
- (51) Koo, J. W.; Duman, R. S. *Proc. Natl. Acad. Sci. U.S.A.* **2008**, *105*, 751–756.
- (52) Theoharides, T. C.; Kempuraj, D.; Tagen, M.; Conti, P.; Kalogeromitros, D. *Immunol. Rev.* **2007**, *217*, 65–78.
- (53) Teague, C. R.; Dhabhar, F. S.; Barton, R. H.; Beckwith-Hall, B.; Powell, J.; Cobain, M.; Singer, B.; McEwen, B. S.; Lindon, J. C.; Nicholson, J. K.; Holmes, E. *J. Proteome Res.* **2007**, *6*, 2080–2093.
- (54) Depke, M.; Fusch, G.; Domanska, G.; Geffers, R.; Volker, U.; Schuett, C.; Kiank, C. *Endocrinology* **2008**, *149*, 2714–2723.
- (55) Ni, Y.; Su, M.; Lin, J.; Wang, X.; Qiu, Y.; Zhao, A.; Chen, T.; Jia, W. *FEBS Lett.* **2008**, *582*, 2627–2636.
- (56) Wang, X.; Zhao, T.; Qiu, Y.; Su, M.; Jiang, T.; Zhou, M.; Zhao, A.; Jia, W. *J. Proteome Res.* **2009**, *8*, 2511–2518.
- (57) Li, Z.-Y.; Zheng, X.-Y.; Gao, X.-X.; Zhou, Y.-Z.; Sun, H.-F.; Zhang, L.-Z.; Guo, X.-Q.; Du, G.-H.; Qin, X.-M. *Rapid Commun. Mass Spectrom.* **2010**, *24*, 3539–3546.
- (58) Zheng, S.; Yu, M.; Lu, X.; Huo, T.; Ge, L.; Yang, J. *Clin. Chim. Acta* **2010**, *411*, 204–209.
- (59) Kiank, C.; Entleutner, M.; Furl, B.; Westerholt, A.; Heidecke, C.; Schutt, C. *Shock* **2007**, *27*, 305–311.
- (60) Kiank, C.; Holtfreter, B.; Starke, A.; Mundt, A.; Wilke, C.; Schütt, C. *Brain, Behav., Immun.* **2006**, *20*, 359–368.
- (61) Cirulli, F.; Pistillo, L.; de Acetis, L.; Alleva, E.; Aloe, L. *Brain, Behav., Immun.* **1998**, *12*, 123–133.
- (62) Esposito, P.; Gheorghe, D.; Kandere, K.; Pang, X.; Connolly, R.; Jacobson, S.; Theoharides, T. C. *Brain Res.* **2001**, *888*, 117–127.
- (63) Zhuang, X.; Silverman, A. J.; Silver, R. *J. Neurobiol.* **1996**, *31*, 393–403.
- (64) Abusaad, I.; MacKay, D.; Zhao, J.; Stanford, P.; Collier, D. A.; Everall, I. P. *J. Comp. Neurol.* **1999**, *408*, 560–566.
- (65) Long, J. M.; Kalehua, A. N.; Muth, N. J.; Calhoun, M. E.; Jucker, M.; Hengemihle, J. M.; Ingram, D. K.; Mouton, P. R. *Neurobiol. Aging* **1998**, *19*, 497–503.
- (66) Long, J. M.; Kalehua, A. N.; Muth, N. J.; Hengemihle, J. M.; Jucker, M.; Calhoun, M. E.; Ingram, D. K.; Mouton, P. R. *J. Neurosci. Methods* **1998**, *84*, 101–108.
- (67) Kempermann, G.; Kuhn, H. G.; Gage, F. H. *Nature* **1997**, *386*, 493–495.
- (68) Kempermann, G.; Kuhn, H. G.; Gage, F. H. *Proc. Natl. Acad. Sci. U.S.A.* **1997**, *94*, 10409–10414.
- (69) Orr, E. L.; Pace, K. R. *J. Neurochem.* **1984**, *42*, 727–732.
- (70) Silverman, A.-J.; Asarian, L.; Khalil, M.; Silver, R. In *Progress in Brain Research*; Ishwar, S. P., Ed.; Elsevier: Amsterdam, The Netherlands, 2002; Vol. 141, pp 315–325.
- (71) Yang, M.; Chien, C.; Lu, K. *Brain Res.* **1999**, *846*, 30–39.
- (72) Larson, A. A.; Thomas, M. J.; McElhose, A.; Kovács, K. J. *Brain Res.* **2011**, *1395*, 30–37.
- (73) Marszalek, P. E.; Farrell, B.; Verdugo, P.; Fernandez, J. M. *Biophys. J.* **1997**, *73*, 1169–1183.
- (74) Ruoss, S. J.; Gold, W. M.; Caughey, G. H. *Biochem. Biophys. Res. Commun.* **1991**, *179*, 140–146.
- (75) Agnati, L. F.; Guidolin, D.; Guescini, M.; Genedani, S.; Fuxe, K. *Brain Res. Rev.* **2010**, *64*, 137–159.
- (76) Feyerabend, T. B.; Weiser, A.; Tietz, A.; Stassen, M.; Harris, N.; Kopf, M.; Radermacher, P.; Moller, P.; Benoist, C.; Mathis, D.; Fehling, H. J.; Rodewald, H. R. *Immunity* **2011**, *35*, 832–844.